Reprinted from "The Proceedings of the Indian Academy of Sciences" Vol. XLV, No. 1, Sec. A, 1957

GENERALISED THEORY OF INTERFERENCE AND ITS APPLICATIONS

Part IV. Interference Figures in Absorbing Biaxial Crystals

BY S. PANCHARATNAM
(*Memoir No. 98 of the Raman Research Institute, Bangalore-6*)

Received April 22, 1957
(Communicated by Sir C. V. Raman)

§ 1. INTRODUCTION

THE interference figures displayed by absorbing biaxial crystals are of some general interest—quite apart from the light they throw on the optics of such media (Voigt, 1902 *a*; Boguslowski, 1914; Pancharatnam, 1955 *b*). The appearance of idiophanic interference rings with no analyser, or with no polariser, or with neither polariser nor analyser, finds no parallel in the field of transparent crystals; these peculiarities arise mainly from the fact that the two waves propagated along any particular direction are in *non-orthogonal* states of elliptic polarisation. Attention has already been directed in the introductions to Parts I and II (Pancharatnam, 1956 *a*, *b*) to some of of these phenomena and their broad explanation. It is sufficient therefore to remark that here we meet with practical instances of some of the most general cases of dissolution, composition, etc., which were theoretically envisaged in those papers on completely and partially coherent pencils. The physical concepts developed there enable us to give a comparatively intelligible explanation to otherwise complex phenomena, and the fruitfulness of these ideas is evidenced by the discovery of certain new phenomena in this field, *e.g.*, the formation of spiral interference figures even with optically inactive crystals (§ 8 *b*).

The general theoretical approach is outlined in Sections 2 and 6 which deal respectively with the two classes of interference phenomena into which the subject may be broadly divided, *viz.*, those exhibited respectively *without* and *with* the aid of an analyser behind the plate—the incident light being either completely polarised, partially polarised or even unpolarised. The concept of partially coherent beams discussed in Part II, apart from giving physical insight into the interference phenomena exhibited when the incident light is unpolarised (§§ 4 and 7), also explains certain new phenomena observed when the incident light is partially polarised (§§ 5 and 8 *b*).

§ 2. GENERAL DISCUSSION OF INTERFERENCE PHENOMENA OBSERVED WITHOUT ANY ANALYSER

In the succeeding sections we shall discuss the interference phenomena exhibited by a plate of an absorbing biaxial crystal without the use of an analyser, when the incident light is either completely polarised (§ 3), unpolarised (§ 4) or partially polarised (§ 5). When a *parallel* beam of unit intensity falls on such a plate it is split into two elliptically polarised streams in the states of polarisation A and B that are propagated without change of form in that direction. Let I_1 and I_2 be the intensities of the component beams, ϕ_1 their initial 'phase difference' at the point of entry into the medium, and γ their mutual degree of coherence (which will be equal to unity only in the case when the incident light is completely polarised). The streams travel through the crystal with different velocities and coefficients of absorption. Emerging from the crystal plate, we therefore have two beams (in states of polarisation A and B) whose intensities are now I_1' and I_2', the 'phase advance' of the first beam over the second being now $\triangle'$, where

$$\left.\begin{array}{l} I_1' = I_1 e_a{}^2; \;\; I_2' = I_2 e_b{}^2 \\ \triangle' = \delta + \phi_1 \end{array}\right\} \qquad (1)$$

the phase retardation introduced by the plate being denoted by δ. These beams can directly interfere with one another, since in general they are in non-orthogonal states of polarisation and are not incoherent. The intensity I obtained on compounding the pencils is given by the general interference formula for beams in different states of polarisation (Part II, eq. 13).

$$I = I_1' + I_2' + 2\gamma \sqrt{I_1' I_2'} \cos \tfrac{1}{2} c \cos \triangle' \qquad (2)$$

where c is the angular separation of the states A and B when represented on the Poincaré sphere.

The variation of I with the direction of propagation may be observed in *convergent* light, using a plate cut normal to an optic axis, each *point* P in the convergent light figure corresponding to a definite *direction* of propagation. For a plate of moderate thickness the retardation δ introduced by the plate increases rapidly as we proceed outwards along directions normal to the curves of constant retardation. The rate of variation of I as we proceed outwards from regions near the optic axis can therefore be taken to be predominantly due to the change in $\triangle'$ (for most regions of the convergent light figure). Hence we should in general expect the appearance of idiophanic interference rings. From what has been said above the curves of minimum intensity occur along directions where the emerging beams destructively interfere, that is, along the curves

$$\triangle' = (2n + 1)\pi$$

or

$$\delta = (2n + 1)\pi - \phi_1 \tag{3}$$

and a measure of the 'visibility' of the fringes (in the sense defined by Michelson) at any point in the convergent light figure is given by

$$V = \gamma \cos \tfrac{1}{2} c \frac{2\sqrt{I_1' I_2'}}{I_1' + I_2'} \tag{4}$$

From (3) we see that the curves of minimum intensity do not occur at the same position as those obtained between crossed polaroids (which occur at $\delta = 2n\pi$); in fact they do not even follow the curves of constant retardation $\delta =$ const., because the initial phase difference ϕ_1 itself varies with direction (since the states A and B vary with direction). In the case of non-active crystals, as we shall see the idiophanic rings in plane polarised light exhibit clearly the first effect but not the second—which may, however, be strikingly seen with the use of circularly polarised light.

Since all the factors in (4) vary *along* a curve $\triangle' =$ const., we should expect the visibility of the rings to be maximum along some particular zone in the field of view—the determination of which is in general very complex since it depends not only on the state of polarisation of the incident light, but also on the thickness of the plate.

The explanation of the appearance of idiophanic rings (in completely polarised, unpolarised or partially polarised light), and of some of their broad characteristics is thus immediately obvious in the present treatment and applies equally well to absorbing biaxial crystals possessing *optical activity*—where the non-orthogonal elliptic vibrations A and B bear no simple relation to one another (Pancharatnam, to be published).

§ 3. Phenomena in Absorbing Biaxial Crystals Using a Polariser Alone

(*a*) *General discussion.*—If completely polarised light be incident on the plate, the component beams into which it is split will be completely coherent. Their intensities I_1 and I_2, and their initial phase difference ϕ_1, may be expressed (see Part I, eqns. 3 and 5 *b*) in terms of the sides of the spherical triangle ABC_1 on the Poincaré sphere—where C_1 represents the state of polarisation of the incident elliptic vibration, and A and B the states of the beams into which it is split.

$$\left.\begin{array}{l} I_1 = \dfrac{\sin^2 \frac{1}{2} a_1}{\sin^2 \frac{1}{2} c}\,; \quad I_2 = \dfrac{\sin^2 \frac{1}{2} b_1}{\sin^2 \frac{1}{2} c} \\ \phi_1 = \pi - \frac{1}{2} E' \end{array}\right\} \tag{5}$$

Here E' is the area of the triangle $C_1'BA$ (measured with the usual sign convention) C_1' being the point opposite to the incident state C_1 (see Fig. 1, text).

The intensity I at the corresponding point in the field of view is obtained by substituting in (2):

$$I = \operatorname{cosec}^2 \tfrac{1}{2} c \{e_a^2 \sin^2 \tfrac{1}{2} a_1 + e_b^2 \sin^2 \tfrac{1}{2} b_1 - 2e_a e_b \sin \tfrac{1}{2} a_1 \sin \tfrac{1}{2} b_1 \cos \tfrac{1}{2} c \cos (\delta - \tfrac{1}{2} E')\} \tag{6}$$

(*b*) *Phenomena in non-active crystals.*—In order to illustrate that our general method of analysis is capable of handling specific cases we shall briefly consider some of the phenomena exhibited by a plate (cut normal to an optic axis) of the optically inactive orthorhombic mineral iolite. We shall refer to the photographs of the different phenomena exhibited by this mineral published in this paper and in a previous paper (Pancharatnam, 1955 *b*, hereafter referred to as P. 2). The idiophanic rings are always absent along the directions where the waves are orthogonally polarised ($\cos \frac{1}{2} c = 0$)—*i.e.*, along the trace of the axial plane. (The axial plane is kept horizontal in all the photographs).

Voigt (*loc. cit.*) has shown that in non-active absorbing biaxial crystals the two elliptically polarised waves A and B propagated along any one direction, have their major axes crossed and have the same ellipticity ϵ (which, according to the usual sign convention, means that they are also described in the *same* sense). Hence on the Poincaré sphere the longitudes of the points A and B differ by π, but their latitudes are both equal to 2ϵ, as drawn in Fig. 2. [See also Pancharatnam, 1955 *a*.] Accordingly we have to substitute $\frac{1}{2} c = \frac{1}{2}\pi - |2\epsilon|$ in (6), for all the cases discussed below.

If the incident light is, say, *left-circularly polarised*, so that the point C_1 now coincides with the upper pole C_l, then we have to substitute in (6): $a_1 = b_1 = \frac{1}{2}\pi - 2\epsilon$; and $\frac{1}{2} E'$ equal to π or zero, according as ϵ is positive or negative. Hence the intensity at any point in the field of view is,

$$I = \frac{1}{2(1 + \sin 2\epsilon)} (e_a^2 + e_b^2 + 2e_a e_b \sin 2\epsilon \cos \delta). \tag{7}$$

The *asymmetry* of the idiophanic rings with respect to the axial plane, which is observable in Fig. 3, Plate I (taken with left-circularly polarised light) is now readily explicable. In the upper half of the figure where the sense of rotation of the ellipses propagated is opposite to that of the incident circularly polarised light, ϵ is negative and hence the minima occur at $\delta = 2\pi$, 4π, etc. (This is verified from the fact that they occur in the same position as in Fig. 1, Plate I, which is obtained when a circular analyser which can cross out the incident light is also introduced.) In the lower half of the figure where ϵ is positive, the minima occur at $\delta = \pi$, 3π, etc. (which is verified from the fact that the fringes are shifted down by half a fringe width relative to those appearing in the upper half of the figure). The expression for I becomes indeterminate at $\epsilon = -\pi/4$, *i.e.*, at the singular axis where *only* a right circular vibration can be propagated *unchanged*. That the emergent intensity is larger than at the other singular axis where the incident light is propagated unchanged, is clearly shown by referring to Fig. 3. This remarkable phenomenon has been theoretically discussed elsewhere (Pancharatnam, 1955 *a*, *b*). When right circularly polarised light is used, the sign of the third term in (7) has to be changed, and the asymmetry about the axial plane will be reversed (see P. 2, Figs. 13 and 14).

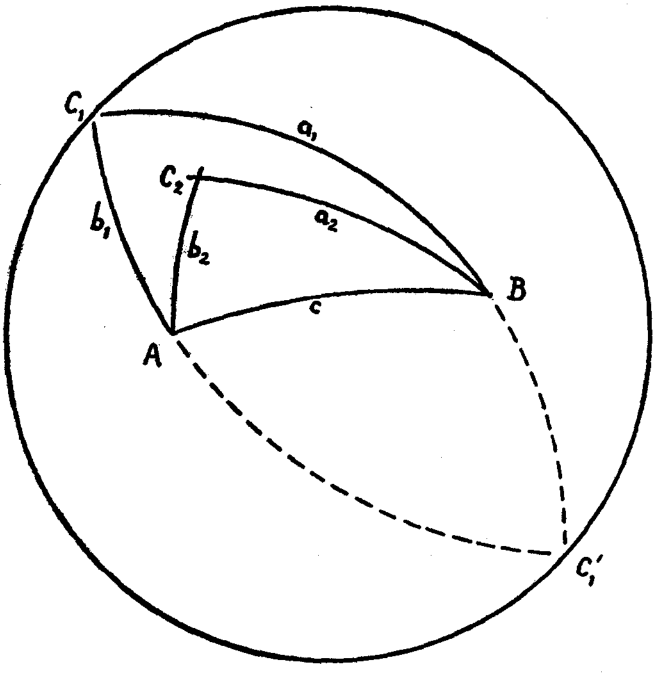

FIG. 1

If the incident light is *plane polarised,* the point C_1 lies on the equator as is drawn in Fig. 2, text. From the figure we see that $b_1 = (\pi - a_1)$ and $E' = -\angle AC_1B$ (since the area E' of the triangle $C_1'BA$ is numerically half the area of the lune of $\angle AC_1B = \hat{C}_1$). Substituting these values in (4), we have

$$I = \operatorname{cosec}^2 \tfrac{1}{2} c \{e_a{}^2 \sin^2 \tfrac{1}{2} a_1 + e_b{}^2 \cos^2 \tfrac{1}{2} a_1 - 2e_a e_b \sin \tfrac{1}{2} a_1 \cos \tfrac{1}{2} a_1 \cdot \cos \tfrac{1}{2} c \cos (\delta + \tfrac{1}{2} \hat{C}_1)\} \tag{8}$$

Let $-\nu$ be the azimuth of the major axis of the faster elliptic vibration with respect to the vibration-direction of the incident light. In directions where the ellipticity is small (so that the points A and B lie near the equator), an approximate formula may be obtained by substitutions $\sin^2 \frac{1}{2} a_1 \simeq \cos^2 \nu$; $\cos^2 \frac{1}{2} a_1 \simeq \sin^2 \nu$; $\sin^2 \frac{1}{2} c \simeq 1$; $\cos \frac{1}{2} c \simeq |2\epsilon|$; and $|\hat{C}_1| = \pi$. We then obtain the approximate formula that is customarily used (Pockels, 1906, p. 423, eq. 9).

$$I = e_a{}^2 \cos^2 \nu + e_b{}^2 \sin^2 \nu + 2\epsilon \sin 2\nu \, e_a e_b \sin \delta \tag{9}$$

Figure 2 of the text shows qualitatively that the last substitution $|\hat{C}_1| = \pi$ will be justified except for directions of propagation where $\nu \simeq 0$, where in any case the interference effects [depending on the last term in (9)], vanish by virtue of the first substitutions. The maxima and minima are thus shifted by *quarter* of a fringe width compared to those obtained between crossed polaroids (see P. 2, Figs. 2 and 9).

To obtain the exact formula for the intensity at any point in the field, we have to use in (8) the exact values of a_1, c and $\hat{C}_1$ which are obtained by spherical trigonometry, from the right-angled triangle AXC_1:

$$\tan \tfrac{1}{2} \hat{C}_1 = \sin 2\nu / \tan 2\epsilon; \quad \cos a_1 = -\cos 2\epsilon \cos 2\nu;$$

$$\sin a_1 \cos \tfrac{1}{2} c = \frac{\cos 2\epsilon \sin 2\nu}{\sin \tfrac{1}{2} \hat{C}_1} \cdot \sin 2\epsilon.$$

It can thus be shown that the approximate formula (9) neglects only the squares and higher powers of the ellipticity ϵ. [Strictly speaking, the idiophanic rings on each side of the axial plane will take the form of the arcs of a spiral (see § 8 *b*) when the polariser is inclined to the axial plane.] It can also be shown that the exact formula deduced by Voigt can be put in the same form as that obtained by the above substitutions.

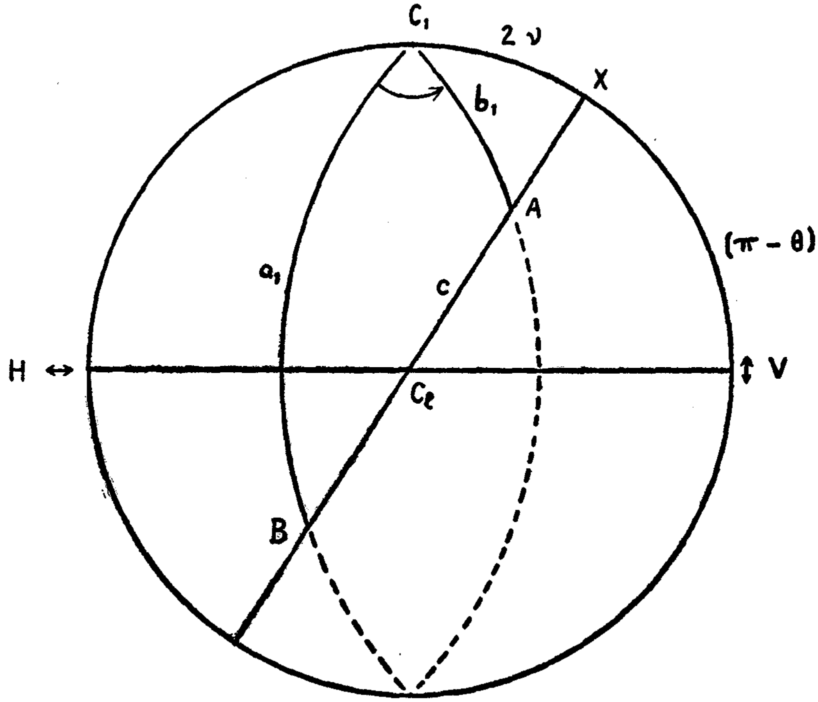

FIG. 2

§ 4. INTERFERENCE PHENOMENA IN ABSORBING BIAXIAL CRYSTALS IN UNPOLARISED LIGHT

It was shown in Part II, § 7, that when unpolarised light is split into two non-orthogonally polarised beams (in the states of polarisation A and B), the component beams are *partially* coherent with one another. The intensities I_1 and I_2 of the component beams, their initial phase difference ϕ_1, and their mutual degree of coherence γ are given by

$$I_1 = I_2 = \tfrac{1}{2}\operatorname{cosec}^2 \tfrac{1}{2}c\,; \;\; \gamma = \cos \tfrac{1}{2}c\,; \;\; \phi_1 = \pi. \tag{10}$$

The intensity I at any point in the field of view, is given by substituting in (2)

$$I = \tfrac{1}{2}\operatorname{cosec}^2 \tfrac{1}{2}\, c\,\{e_a{}^2 + e_b{}^2 - 2e_a e_b \cos^2 \tfrac{1}{2}\, c \cos \delta\} \tag{11}$$

The interference effects observed (Fig. 5, Plate I) are extremely feeble since they depend on the *square* of the factor $\cos \frac{1}{2}c$, which becomes appreciable only in immediate neighbourhood of the singular axes. What is actually seen—both in the optically active crystal amethyst and in the inactive crystal iolite—is the occurrence of the first minimum on either side of the optic axis as two dark spots at the terminii of the Brewster's brushes. These minima should occur at $\delta = 2\pi$; and in the case of iolite (Fig. 5, Plate I), this is confirmed by the fact that they occur at the same position as the first minima obtained between crossed polaroids (Fig. 6, Plate I)—as may be verified by measurement (see also § 5 *b*).

§ 5. INTERFERENCE PHENOMENA IN PARTIALLY POLARISED LIGHT

(*a*) *Incident light partially circularly polarised.*—Just as the addition of two incoherent *non-orthogonally* polarised beams results in a partially polarised beam, so also when a partially polarised beam is split into two non-orthogonally polarised beams it is possible under certain circumstances for the component beams to be completely incoherent with one another. Hence with partially polarised light incident on a plate of an absorbing biaxial crystal, it should be possible under certain conditions for the interference fringes to completely vanish near some particular regions in the convergent light figure (observed with or without an analyser).

Fig. 7, Plate II of this paper shows a photograph of this curious phenomenon as exhibited by a plate of iolite when the incident light is partially circularly polarised. An analysing polaroid was set behind the plate with its vibration direction perpendicular to the axial plane. The partially left-circularly polarised light was obtained by passing partially plane polarised light—emerging from a pile of plates—through a quarter-wave plate.

For analysing the phenomenon we shall use the representation discussed in Part II whereby any beam (completely or partially polarised) is characterised by its total intensity and by a 'Stokes vector' drawn from the centre of the Poincaré sphere; the length of the vector and its orientation (*i.e.*, point of intersection with the sphere) give respectively the intensity and state of polarisation, of the 'polarised fraction' of the beam. Let us denote by $\mathbf{S}$ the vector representing the incident partially left-circularly polarised light (of unit intensity and degree of polarisation p); and let $\mathbf{S}_1$ and $\mathbf{S}_2$ be the Stokes vectors representing the component beams—completely polarised in states A and B—into which the incident light is split. Then obviously

$$\mathbf{S} = p\mathbf{C}_l;\ \mathbf{S}_1 = \mathrm{I}_1\mathbf{A};\ \mathbf{S}_2 = \mathrm{I}_2\mathbf{B} \tag{12}$$

where $\mathbf{C}_l$, $\mathbf{A}$, $\mathbf{B}$ are unit vectors directed towards the points C_l, A and B respectively (see Fig. 3, text). The intensities I_1 and I_2 of the component beams must be equal to one another, since the states A and B are symmetrically situated with respect to the pole C_l, for a non-active crystal; they are given by eq. 21 of Part II,

$$\mathrm{I}_2 = \mathrm{I}_1 = \tfrac{1}{2}(1 - \mathbf{S}\cdot\mathbf{B})\operatorname{cosec}^2 \tfrac{1}{2}c$$
$$= \tfrac{1}{2}(1 - p \sin 2\epsilon)/\cos^2 2\epsilon \tag{13}$$

It was shown in Part II, § 6, that when two completely polarised beams $\mathbf{S}_1$ and $\mathbf{S}_2$ are combined to give a resultant beam $\mathbf{S}$, then

$$\mathbf{S} = \mathbf{S}_1 + \mathbf{S}_2 + \mathbf{S}_{12}$$

where $\mathbf{S}_{12}$ is a vector arising from the interference of the component beams, and by determining which we can in the present case calculate the degree of coherence γ and the effective phase difference ϕ_1 between the component beams. Substituting from (12) and referring to Fig. 3, text, we have

$$\mathbf{S}_{12} = (p - 2\mathrm{I}_1 \sin 2\epsilon)\,\mathbf{C}_l$$

or from (13)

$$\mathbf{S}_{12} = 2\mathrm{I}_1 \cdot \frac{p - \sin 2\epsilon}{1 - p \sin 2\epsilon}\,\mathbf{C}_l \tag{14}$$

Since $\mathbf{S}_{12}$ is coplanar with $\mathbf{S}_1$ and $\mathbf{S}_2$ it follows from the geometric construction for $\mathbf{S}_{12}$ given in Part II, Fig. 2, that (*a*) the length of the vector $\mathbf{S}_{12}$ is equal to $2\gamma\sqrt{\mathrm{I}_1\mathrm{I}_2}$, and (*b*) the effective phase difference between the component beams is zero or π according as $\mathbf{S}_{12}$ bisects the interior or exterior angle between $\mathbf{S}_1$ and $\mathbf{S}_2$.

The appearance of the figure presented (either without any analyser or with an analyser set along or perpendicular to the axial plane) may now be understood in terms of the variation of the ellipticity of the waves over the region covered by the convergent light figure. (See Voigt, 1902 ***a***; also P. 2, Fig. 1.)

In the lower half of the figure where ϵ is negative (because of the manner in which the plate was set), we see from (14) that the degree of coherence never vanishes and the initial phase difference is π. On the other hand, in the region above the trace of the axial plane the degree of coherence vanishes where $\mathbf{S}_{12} = 0$, *i.e.*, where $\sin 2\epsilon$ is equal to the degree of polarisation p. Towards the interior of this region the ellipticity ϵ becomes greater and the initial phase difference ϕ_1 between the component beams is π; while towards the exterior of this region $\sin 2\epsilon < p$ and accordingly the initial phase difference jumps to zero. Thus in Fig. 7, Plate II, as we proceed upwards from the optic axis, the first ring is clearly seen (appearing at the same distance as that in the lower half of the figure); further on *the rings disappear* and then reappear with *a shift of half a fringe width* compared ot those in the lower half of the figure—thus confirming our theoretical deductions. The use of an analyser behind the crystal plate increases the clarity of the interference phenomena by resolving the beams into the same state of polarisation before making them interfere. This does not affect the main conclusions of our discussion.

(*b*) *Incident light partially plane polarised.*—When a partially polarised beam is decomposed into two non-orthogonally polarised beams, it may be shown that the effective phase difference between the component beams is *not* independant of the degree of polarisation. Let us suppose that the incident light of degree of polarisation p is partially *plane* polarised in any state C_1 (Fig. 2, text). It would then be represented by a vector $\mathbf{S}$ of length p directed towards C_1. The initial phase difference ϕ_1 between the component beams in the states of polarisation A and B is given by Part II, eqns. 22 *a* and 23 *a*:

$$\tan \phi_1 = V'/U', \quad (\tfrac{1}{2}\pi \leq \phi_1 \leq 3\pi/2)$$

where

$$V' = S_z \operatorname{cosec} \tfrac{1}{2} c; \quad U' = -\cos \tfrac{1}{2} c \operatorname{cosec}^2 \tfrac{1}{2} c$$

and where the positive z direction is in the direction of the vector $\mathbf{A} \times \mathbf{B}$. Considering the case when the beam is incident on an optically inactive absorbing crystal (*e.g.*, iolite) we will have (see Fig. 2, text)

$$\tan \phi_1 = p \sin 2\nu / \tan 2\epsilon = p \tan \tfrac{1}{2} \hat{C}_1 \tag{15}$$

where the symbols have the same meaning as previously (§ 3 *b*). Thus as the degree of polarisation is increased from zero the initial phase difference ϕ_1 alters continuously from π to $(\pi + \tfrac{1}{2}\hat{C}_1)$.

This was experimentally demonstrated by partially polarising the incident light with its vibration parallel to the axial plane of iolite by the use of a pile of plates, and observing the convergent light figure without the use of an analyser. Starting with the light more or less completely polarised (P. 2, Fig. 6), the degree of polarisation was gradually decreased to zero (by turning the pile of plates about an axis perpendicular to the axial plane). It was then observed that not only did the rings become less distinct at the border of the figure, but at the same time they moved slightly *outwards*, till finally when the light was unpolarised what was left were the minima in the Brewster's brushes.

Incidentally the above experiment demonstrates clearly a fact which follows from the theoretical discussion of §§ 3 and 4, namely, that the minima in the Brewster's brushes do not exactly coincide with those observed when the light is polarised parallel to the axial plane. This fact was not realized in a previous paper (P. 2), though a measurement on the photographs (Figs. 5 and 6) published in that very paper confirms the above result.

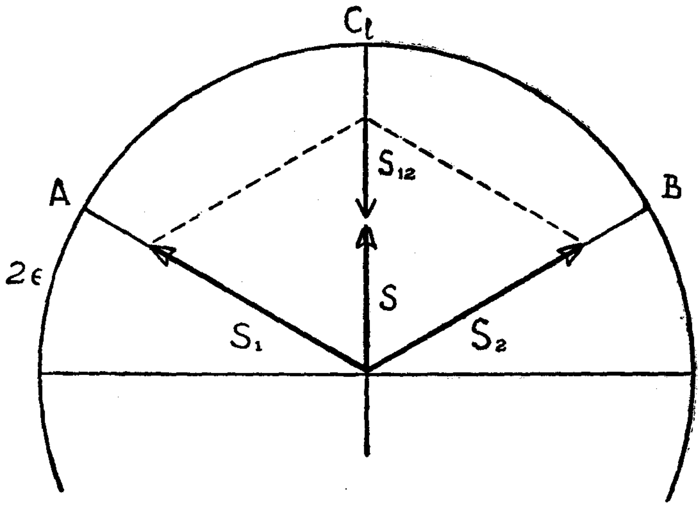

FIG. 3

§ 6. GENERAL DISCUSSION OF INTERFERENCE PHENOMENA INVOLVING USE OF AN ANALYSER

In the succeeding sections we shall discuss the interference phenomena exhibited in convergent light by a crystal plate when an analyser C_2 (which transmits light of elliptic polarisation C_2) is used behind the crystal plate—the incident light being either unpolarised (§ 7), or completely or partially polarised (§§ 8, 9). As before let I_1' and I_2' be the intensities of the two pencils (in the states of polarisation A and B respectively) which emerge from the crystal plate along any particular direction, their degree of coherence being γ, and the effective phase advance of the first beam over the second being Δ'. The analyser transmits the resolved components of these beams in the state of polarisation C_2, and these components can interfere with one another. Let the intensities of the resolved components be I_1'' and I_2'', their effective phase difference being Δ''. These may be written down in terms of the spherical triangle ABC_2 (Fig. 1, text) using the results of Part I, § 8, and Part II, § 4.

Writing $\Delta'' = \Delta' + \phi_2$, we have

$$\left.\begin{aligned} &I_1'' = I_1' \cos^2 \tfrac{1}{2} b_2; \quad I_2'' = I_2' \cos^2 \tfrac{1}{2} a_2; \\ &\phi_2 = -\tfrac{1}{2} E_2 \end{aligned}\right\} \qquad (16)$$

where E_2 is the area of the triangle ABC_2. The phase diffrence Δ'' between the two finally interfering beams is thus the sum of three terms:

$$\Delta'' = \phi_1 + \delta + \phi_2 \tag{17}$$

where ϕ_1 is the initial phase difference—'introduced in the process of decomposition'—between the pencils at the first surface of the plate, δ is the phase retardation introduced by the plate, and ϕ_2 may be called the phase difference introduced in the process of analysation.

The resultant intensity I transmitted by the analyser is given by the formula for the interference of two beams in the same state of polarisation, having a degree of coherence γ.

$$I = I_1'' + I_2'' + 2\gamma \sqrt{I_1'' I_2''} \cos \Delta'' \tag{18}$$

The general arguments following eq. 2 may be applied *mutatis mutandis* in the present case. The appearance of interference figures with an analyser is therefore to be expected whether the incident light is unpolarised or completely or partially polarised. The curves of minimal intensity follow the curves where $\Delta'' = (2n + 1)\pi$. Since Δ'' is given by (17) these curves will not in general follow the curves of constant retardation $\delta = \text{const.}$; this is because *the sum of the phase differences* ϕ_1 *and* ϕ_2 (which are introduced by the processes of resolution and analysation respectively) *is not constant, but is itself a function of the direction of propagation.* This is the true physical reason why the interference figures in quartz, and, as we shall see, also in iolite, can under suitable conditions even take the form of spirals.

§ 7. IDIOPHANIC RINGS WITH AN ANALYSER ALONE

The idiophanic rings in the present case (with the incident light unpolarised) are of the same clarity as those obtained with a polariser *alone* in front of the plate. In the present case, however, the intensity I at any point in the field of view is obtained by substituting the values given by (10) in (18):

$$\begin{aligned} I = \tfrac{1}{2} \operatorname{cosec}^2 \tfrac{1}{2} c \, \{ & e_a{}^2 \cos^2 \tfrac{1}{2} b_2 + e_b{}^2 \cos^2 \tfrac{1}{2} a_2 \\ & - 2 e_a e_b \cos \tfrac{1}{2} a_2 \cos \tfrac{1}{2} b_2 \cos \tfrac{1}{2} c \cos (\delta - \tfrac{1}{2} E_2) \} \end{aligned} \tag{19}$$

In view of the fact that this expression differs from (6), an explanation is required as to why the idiophanic rings seen with the polaroid set either before or after the plate do *not* differ in the case of non-active absorbing crystals like iolite (compare Figs. 8 and 10 of P. 2). This equivalence is not a general result but a consequence of the peculiar fact that in non-active crystals the two ellipses propagated along any direction have their major axes crossed and their ellipticities equal. In such a case (see Fig. 2, text) we have $a = (\pi - b)$ and $E = E'$, so that the expressions (6) and (19) become equal. However in the case of optically active absorbing crystals it can be shown that the states A and B do not bear this simple relation to one another (work to be published), and in such a case the idiophanous figure presented with a polaroid set in front of the crystal should not be the same as that obtained with the polaroid set behind the plate in the same position. This difference has been observed in the case of amethyst.

That the effects presented with a polariser C alone are *in general* not the same as those obtained with an analyser C alone, may be confirmed even in the case of inactive absorbing biaxial crystals if C represents a state of elliptic polarisation. Thus the idiophanic rings with a left-circular analyser (Fig. 4, Plate I) are not the same as with a left-circular polariser (Fig. 3, Plate I), but should be the same as the figure seen with a *right*-circular polariser (as may be shown by comparing eqns. 6 and 19]). This latter proposition has also been confirmed experimentally in iolite.

§ 8. Interference Figures in Absorbing Biaxial Crystals Between Polariser and Analyser

(*a*) *General discussion.*—When *completely* polarised light of unit intensity in the state of polarisation C_1 is incident on a plate of an absorbing biaxial plate, and an analyser C_2 is used behind the plate, the intensities I_1'' and I_2'' and the difference in phase Δ'' of the two pencils transmitted by the analyser along any particular direction are given by substituting in (16) from (5) and (1):

$$I_1'' = \frac{\sin^2 \frac{1}{2} a_1 \cos^2 \frac{1}{2} b_2}{\sin^2 \frac{1}{2} c} \cdot e_a^2; \quad I_2'' = \frac{\sin^2 \frac{1}{2} b_2 \cos^2 \frac{1}{2} a_2}{\sin^2 \frac{1}{2} c} \, e_b^2$$

$$\Delta'' = \delta + \pi - \tfrac{1}{2}(E_1' + E_2)$$

where, it may be noted, $(E_1' + E_2)$ is the area of the spherical quadrilateral $C_1'BC_2A$ (see Fig. 1, text).

The resultant intensity I_2 transmitted by the analyser is given by the formula (18) for the interference of two completely coherent pencils in the same state of polarisation. Hence

$$I = \operatorname{cosec}^2 \tfrac{1}{2} c \, [e_a^2 \sin^2 \tfrac{1}{2} a_1 \cos^2 \tfrac{1}{2} b_2 + e_b^2 \sin^2 \tfrac{1}{2} b_1 \cos^2 \tfrac{1}{2} a_2 - 2 e_a e_b \sin \tfrac{1}{2} a_1 \sin \tfrac{1}{2} b_1 \cos \tfrac{1}{2} a_2 \cos \tfrac{1}{2} b_2 \cos \{\delta - \tfrac{1}{2}(E_1' + E_2)\}] \tag{20}$$

The equation for the case of transparent crystals (Part III), is obviously a particular case of the above.

For the particular case when polariser and analyser are crossed we have $a_1 = \pi - a_2$; $b_1 = \pi - b_2$ and $(E_1' + E_2) = 0$. Hence

$$I = \frac{\sin^2 \frac{1}{2} a_1 \sin^2 \frac{1}{2} b_1}{\sin^2 \frac{1}{2} c} (e_a{}^2 + e_b{}^2 - 2e_a e_b \cos \delta) \tag{21}$$

We see therefore that—independant of the orientation of the crossed states C_1 and C_1'—the minima of the ring system occur at $\delta = 2\pi$, 4π, etc., and that the rings are seen most clearly along the zone where the absorption coefficients of the two waves are equal, or $e_a = e_b$ (see Figs. 1, 2 and 6, Plate I).

We can now easily show that the interference figures exhibited between crossed nicols by a plate of an absorbing biaxial crystal *not* possessing optical activity, will be unaltered if the polariser and analyser are interchanged. In such a medium (as we have seen at the end of § 3 *b*) the states of polarisation A and B of the waves propagated in any direction are such that when the incident light is *linearly* polarised we will have $a_1 = \pi - b_1$ (see Fig. 2, text). The effect of interchanging analyser and polariser is then got by changing a_1 to $\pi - a_1$ and b_1 to $\pi - b_1$ and such a change will leave the expression (21) for the emergent intensity unaltered.

It is to be noted however that such an interchange of the crossed nicols could alter the expression for the emergent intensity, if the points A and B are any two general points on the sphere—a situation which occurs in optically active absorbing crystals; the alteration of the observed interference figure on interchanging the crossed nicols has been observed in the case of amethyst (work to be published). That the interchange of the crossed polariser and analyser will in general alter the interference figure may be observed even in the *non*-active crystal iolite provided the incident light is not linearly polarised. This may be seen from the photographs (1) and (2) in which one has been taken between a left-circular polariser and a right-circular analyser, while the other has been taken between a right-circular polariser and a left-circular analyser; the difference between the two figures is small but striking and is mainly in the shift in the position of the eccentric spot from the upper to the lower singular axis.

(*b*) *Spiral figures in inactive absorbing crystals.*—It was observed that when the incident light is plane polarised at an angle of, say, 45° to the axial plane, and a circular analyser is used behind the crystal plate, the interference figure takes a spiral form in the centre of the field of view (Figs. 10 and 11, Plate II). If the incident light is only *partially* plane polarised, the kinks occurring along the vertical line of the field of view become less marked, and several convolutions of the spiral can be clearly traced (Figs. 8 and 9, Plate II).

On the Poincaré sphere (Fig. 2, text) let the horizontal direction (which is also the trace of the axial plane) be represented by H. We shall first treat the case when the analyser is a left-circular analyser C_l, and the state of maximum polarisation of the incident partially plane polarised light is inclined at an angle of $-45°$ to the axial plane and hence represented by the point C_1 on the Poincaré sphere. Any point P in the field of view may be specified by its polar co-ordinates (r, θ) with respect to a horizontal line, and corresponds to a particular direction of propagation in the crystal. Except for points very close to the optic axis, we may take $\frac{1}{2}\theta$ and $(\frac{1}{2}\pi - \frac{1}{2}\theta)$ as the aximuths with respect to the axial plane of the major axes of the faster and slower elliptic vibrations (A and B) propagated in the direction P, their common ellipticity ϵ being given by

$$\epsilon = (\mathrm{K}/2\delta) \sin \theta \tag{22}$$

where K is proportional to the dichroism along the optic axis (see Pockels, *loc. cit.*, p. 425, eq. 13). On the Poincaré sphere, A and B will then have the common latitude 2ϵ and longitudes θ and $(\pi - \theta)$ respectively as indicated in Fig. 2, text. According to (17), the phase difference Δ'' between the resolved components transmitted by the analyser in the direction $\mathrm{P}(r, \theta)$ exceeds the retardation δ introduced by the plate by an angle ϕ,

$$\Delta'' = \delta + \phi, \tag{23}$$

and we have to show that the locus of the direction for which these beams destructively interfere $[\Delta'' = (2n + 1)\pi]$, forms a spiral. The retardation δ of the plate is proportional to the radius vector r, $(\delta = \beta r)$, for regions not too close to the optic axis, and it remains to express ϕ as a function of the direction of propagation. From (16) we have,

$$\phi = \phi_1 - \tfrac{1}{2}\,\mathrm{E}_2 \tag{24}$$

Since E_2 is the area of the triangle ABC_l we have $\frac{1}{2}\,\mathrm{E}_2 = \pi$ for points above the axial plane, and $\frac{1}{2}\,\mathrm{E}_2 = 0$ for points below. The value of the initial phase difference ϕ_1 is given by (15):

$$\tan \phi_1 = -\,p \cos \theta / \tan 2\epsilon; \qquad (\pi/2 \leq \phi_1 \leq 3\pi/2) \tag{25}$$

Substituting from (22), we have, on neglecting the squares and higher powers of ϵ,

$$\tan \phi_1 = (p/\mathrm{K})\, \delta \cot \theta \tag{26}$$

From a consideration of equations 26, 23 and 24 we easily obtain the following result. As we proceed along the circle $\delta = (2n + \frac{1}{2}\pi)$ described about the optic axis, the phase retardation Δ'' between the interfering pencils (transmitted by the analyser) falls short of the value $(2n + 1)\pi$ by an angle which *increases continually* with the aximuth θ, and which in fact becomes equal to θ at $\theta = m\pi/2$. In order therefore to plot the curve $\Delta'' = (2n + 1)\pi$ (condition for destructive interference), we have to increase the radii vectors of the circular curve $\delta = (2n + \frac{1}{2})\pi$ by amounts which increase continuously with the polar angle θ, the radius vector of this curve at the plolar angles $\theta = m\pi/2$ taking the values corresponding to $\delta = (2n + \frac{1}{2})\pi + \frac{1}{2}m\pi$. The curves of minimum intensity thus obtained form a continuous spiral which is described in an anticlockwise or left-handed sense (Fig. 8, Plate II). It may be easily shown that the curve of minimum intensity is wrapped round the curve of maximum intensity, the one being obtained from the other by a rotation of 180° about an axis normal to the plane of the figure.

Fig. 10, Plate II, illustrates that a left-handed spiral is still obtained even when a *right*-circular analyser is used, the plane of maximum polarisation of the incident light being the same as in Fig. 8 (though the incident light is now completely polarised). This is not really surprising, because when a right-circular analyser is used, the only difference is that the value of $(-\frac{1}{2}E_2)$—the phase retardation introduced by the process of analysation—differs by π from the corresponding value when a left-circular analyser is used; so that what was a curve of maximum intensity with a left-circular analyser becomes now a curve of minimum intensity.

If, however, the incident light has its plane of maximum polarisation turned through 90°, so that it is inclined at $+45°$ to the axial plane, it may be shown, by going through the theoretical explanation of the spiral figure, that the sense of description of the spirals will be reversed (being obtained by reflection about a plane perpendicular to the axial plane). Figs. 9 and 11 show the right-handed spirals thus obtained with the incident light respectively partially and completely polarised—the former figure being obtained with a left-circular analyser and the latter with a right-circular analyser.

Along the spiral we have $d\Delta'' = 0$, so that the spiral will be given by

$$\frac{dr}{d\theta} = -\frac{\partial\Delta''}{\partial\theta}\Big/\frac{\partial\Delta''}{\partial r}$$

Writing $\delta = \beta r$ and $(p/\mathrm{K}) = a$, it may be shown by using (23), (24) and (26) that

$$\frac{dr}{d\theta} = \frac{ar}{\sin^2\theta + a^2\beta^2 r^2 \cos^2\theta + a \sin\theta \cos\theta}$$

so that at $\theta = 0$,

$$\left(\frac{dr}{d\theta}\right)_1 = \frac{\mathrm{K}}{p\beta^2 r}$$

and at $\theta = \frac{1}{2}\pi$,

$$\left(\frac{dr}{d\theta}\right)_2 = \frac{pr}{\mathrm{K}}.$$

Thus as the arm of the spiral turns from a horizontal to a vertical position the increase in its length from $r = (2n + \frac{1}{2})\,\pi/\beta$ to $r = (2n + 1)\,\pi/\beta$ does not take place uniformly. Along the horizontal diameter of the figure the increase in the arm of the spiral per unit increase of the polar angle is inversely proportional to the radius of the spiral and *to the degree of polarisation*, while along the vertical diameter it is directly proportional to the same factors. We have thus explained the fact that as the degree of polarisation is raised, the successive arcs of the spiral approximate more and more towards circular arcs along the horizontal diameter while they become more and more kinked along the vertical zone.

The author owes a debt of gratitude to Prof. Sir C. V. Raman, F.R.S., N.L., but for whose encouragement the present work could not have been undertaken.

§ 9. Summary

Phenomena—involving the interference of polarised light—displayed by crystalline plates (in parallel or convergent light) may be given a general method of analysis, using the physical concepts developed in Parts I and II. The subject is discussed under two main heads: the interference phenomena exhibited *without* and *with* the aid of an elliptic analyser behind the crystal plate—the former involving the interference of beams in different non-orthogonal states of elliptic polarisation. The cases when the incident light is either unpolarised, partially polarised, or completely polarised are all discussed—the concept of partially coherent beams finding fruitful applications in the first two cases.

Illustrative photographs of the interference figures in convergent light shown by the optically inactive mineral iolite accompany the paper. Parti-

cular mention may be made of the interference figure with the incident light partially circularly polarised—showing the fading away of the ring system (due to incoherence) at a particular region in the figure; also of the *spiral* interference figures which are observed between a plane polariser and a circular analyser—even though the crystal is optically inactive.

REFERENCES

Boguslowski, S.	.. *Ann. der Physik.*, 1914, **44**, 1084.
Pancharatnam, S.	.. *Proc. Ind. Acad. Sci.*, 1955 *a, b*, **42 A**, 86, 235.
————	.. *Ibid.*, 1956 *a, b*, **54 A**, 247, 398.
Pockels	.. *Lehrbuch der Kristalloptik*, Teubner, 1906.
Voigt	.. *Ann. Phys.*, 1902 *a*, **9**, 367.
————	.. *Phil. Mag.*, 1902 *b*, **4**, 90.

DESCRIPTION OF PLATES

All the photographs show the optic axial interference figures exhibited in convergent light by the absorbing biaxial mineral, iolite, the axial plane being horizontal. Figures 5, 6 and 7 were taken with a much denser specimen than that used for the other photographs.

FIG. 1. Left-circular polariser and right-circular analyser: lower singular axis extinguished.

FIG. 2. Right-circular polariser and left-circular analyser: upper singular axis extinguished.

FIG. 3. Left-circular polariser *alone*: dark rings in lower half of the figure correspond to bright rings in upper half, and the lower singular axis appears darker than the other.

FIG. 4. Left-circular analyser *alone*: asymmetry with respect to the axial plane is reversed, compared to Fig. 3.

FIG. 5. Brewster's brushes with neither polariser nor analyser: minima at tip of brushes are at the same distance as first dark ring in Fig. 6.

FIG. 6. Crossed polaroids: vibration directions along and perpendicular to axial plane.

FIG. 7. Incident light partially left-circularly polarised, and linear analyser with vibration-direction vertical: in the upper half of the figure, the ring system fades away near second and third rings, and reappears further out with a shift of half a fringe width.

FIGS. 8–9. Left-circular analyser, incident light *partially* plane polarised with vibration at $-45°$ and $+45°$ respectively, with respect to axial plane: note the difference in the handedness of the spiral in the two cases.

FIGS. 10–11. Right-circular analyser, incident light *completely* plane polarised, with vibration at $-45°$ and $+45°$ respectively, with respect to axial plane: kinks along the vertical diameter are conspicuous compared to Figs. 8 and 9.

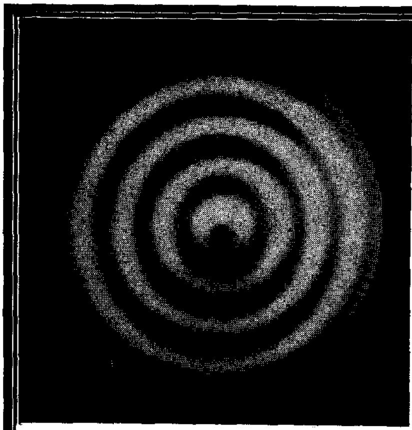

FIG. 1

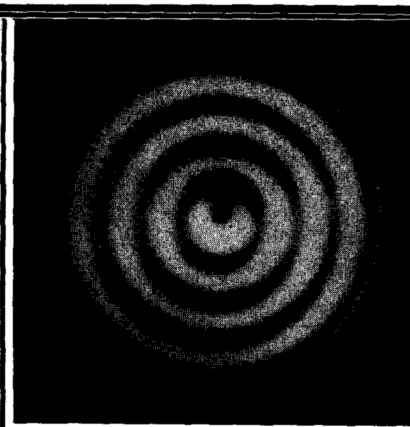

FIG. 2

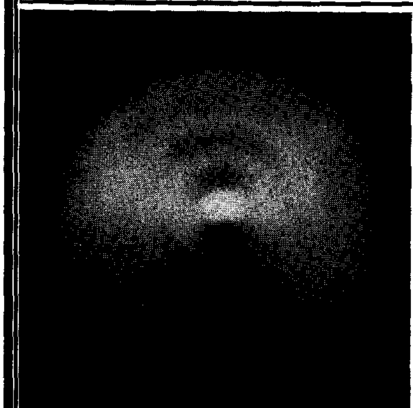

FIG. 3

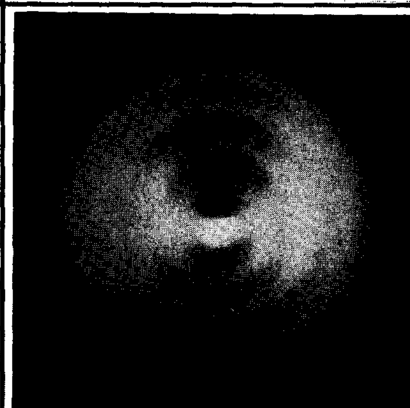

FIG. 4

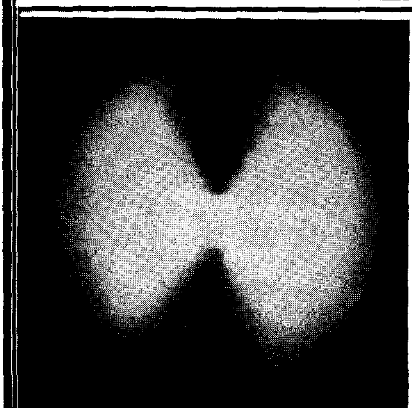

FIG. 5

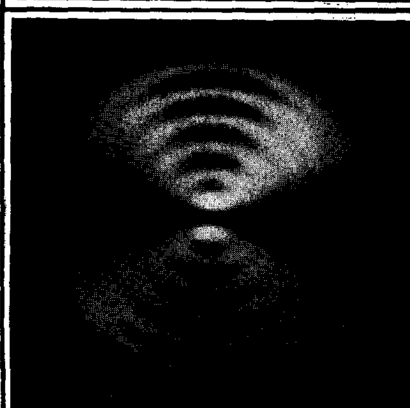

FIG. 6

FIG. 7

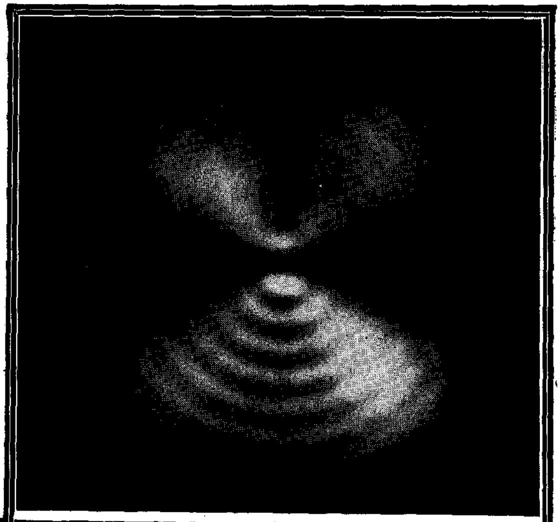

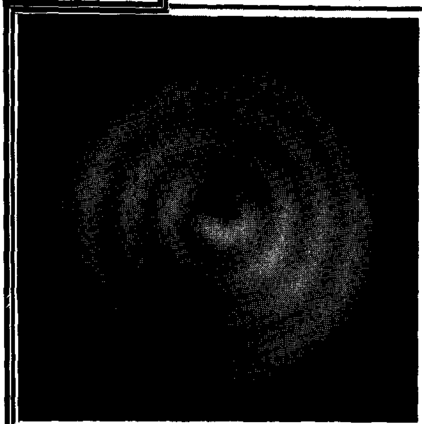

FIG. 8

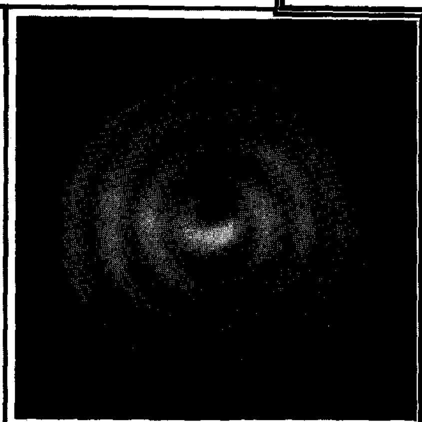

FIG. 9

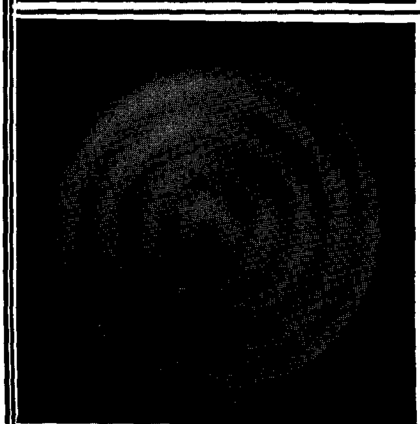

FIG. 10

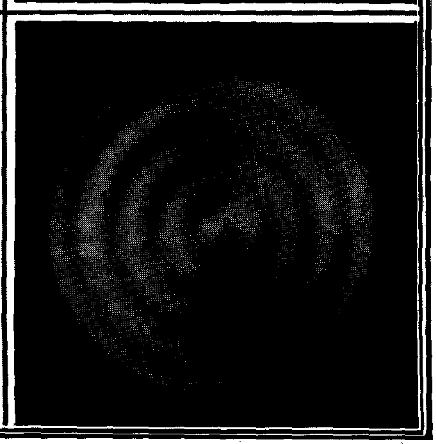

FIG. 11